Butyl-methylimidazolium functionalized resorcinol-formaldehyde resins: synthesis, properties, and applications to methylene blue removal

Martin Tiano, Sara Asad, Ning Zhang, Selene Charlemont, Elsa Manseur, Stéphane Daniele

Butyl-methylimidazolium functionalized resorcinol-formaldehyde resins: synthesis, properties, and applications to methylene blue removal

Martin Tiano,*[a,b] Sara Asad,[b] Ning Zhang,[b] Elsa Manseur,[b] Selene Charlemont,[b] Stéphane Daniele,*[b]

Two new imidazolium-functionalized resorcinol-formaldehyde resins RFs were synthesized, using butyl-methyl imidazolium resorcinate [C_1C_4Im][Res] as a new precursor or using a post-functionalization method. During its synthesis, [C_1C_4Im][Res] spontenaously co-crystallizes with resorcinol (in a 1 : 1 stoichiometry): the crystal structure shows H-bonds between resorcinol and resorcinate, and rarely observed π^+-π^- and C-H - π interactions between imidazolium ring and resorcinate. New RFs presented substantial decreases of the band gap compared to unmodified RF (from 2.0 eV to 1.72 eV). The use of [C_1C_4Im][Res] significantly improves particle size uniformity compared to unmodified RF, whereas the post-functionalization method partially degrades their structure. As RF, the two new resins efficiently catalyse the photodegradation of the methylene blue cation, and the post-functionalised resin has excellent adsorption properties for this dye.

Introduction

Used as a glue for more than 70 years, resorcinol-fromaldehyde resins (RFs) are inexpensive organic polymers synthesized by condensation between formaldéhyde and resorcinol. They are now widely used as adhesives,[1] for hydrogels and aerogel preparation[2,3]. Pioneering work carried out by Zhang *et al.*[4] in 2015 let to the discovery of semiconductive and photocatalytic properties of RFs, and since then, various works highlighted the efficiency of RFs for photodegradation of organic pollutants,[4–9], water oxidation[4], enzyme-like activities[10,11], H_2O_2 production.[9,12–18]. Efforts have been made to control the semiconductive properties and morphology of RF resins, by varying synthetic conditions, tailoring, organic or metal doping.[4–11,15–20] Notably, ionic liquids (ILs) has been used as media for synthesis, or as tailoring agents. More over, Liang *et al.* proposed in 2013 a new material formed by the copolymerisation of acidic ionic liquid oligomers and RF, and its application to acetalization catalysis.[21] But, to our konwledge, no other attempt to functionalize RFs particles with ionic structures has been proposed yet. We propose here to use a ionic liquids synthetic methodology to modify RF composition. The "dimethylcarbonate route" refers to a well-known strategy for a green and efficient ionic liquids synthesis, that lead to the formation of new ion pairs through a metathesis reaction between an methylcarbonate-based ionic liquids ([Cation][$MeOCO_2$]) and an protic precursor (AH) and volatile compounds (MeOH and H_2O).[22]

$$[\text{Cation}][\text{MeOCO}_2] + \text{AH} \longrightarrow [\text{Cation}][\text{A}] + \text{MeOH} + \text{H}_2\text{O}$$

That synthetic route has been used for the synthesis of more than 100 different ionic liquids, but also for TiO_2 particles functionalization,[23] and ionomer synthesis.[24].

Since both resorcinol and RF particles exhibit protic sites (aromatic hydroxyl groups), we therefore propose to use this methodology to pre- or post-functionalize RF resins. The pre-functionalization consists first in the synthesis of the new ionic compound butyl-methylimidazolium resorcinate [C_1C_4Im][Res] from commercial butyl methylimidazolium methylcarbonate [C_1C_4Im][$MeOCO_2$] and resorcinol, and then use it as precursor for the polycondensation with formaldehyde to obtain C_1C_4Im/RF (Fig. 1, a). The post functionalization of RF consists in the direct reaction of [C_1C_4Im][$MeOCO_2$] with the RFs to obtain C_1C_4Im@RF (Fig. 1, b).

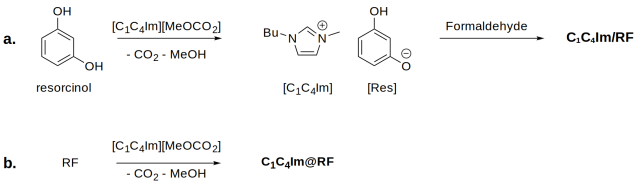

Figure 1. Pre-functionalization strategy (a) and post-functionalization strategy (b) for [C_1C_4Im]-functionalized-RF resins.

[a] Dr. M. Tiano*
Laboratoire de Chimie, École Normale Supérieure de Lyon, CNRS UMR 5182, 46 Allée d'Italie, F-69364 Lyon, France
E-mail: martin.tiano@ens-lyon.fr

[b] Dr. M. Tiano*, Dr. S. Asad, N. Zhang, E. Manseur, S. Charlemont, S. Daniele*
Laboratory of Catalysis, Polymerization, Processes and Materials (CP2M), CNRS UMR 5128, Institut de Chimie de Lyon, Université Claude Bernard Lyon 1, ESCPE Lyon, 43 Bd du 11 Novembre 1918, F-69616 Villeurbanne, France.
E-mail: stephane.daniele@univ-lyon1.fr

1. Experimental

1.1. Materials

Formaldehyde solution (37 % wt. in water), resorcinol, methylene blue and solvents were purchased from Sigma-Aldrich.
1-Butyl-3-methylimidazolium methylcarbonate, 30 % in MeOH was purchased from Iolitec (Germany). All chemicals were used as received.

1.2. Characterizations

UV-Visible spectra were collected on PerkinElmer Lambda 365 using an integrating sphere. Energy gap obtained by Tauc method. [25]
Single crystal X-Ray diffraction was performed on XtaLAB Synergy, Dualflex, HyPix-Arc 100 diffractometer.
Solution NMR spectra ((^{1}H and ^{13}C) were recorded on an Avance-300 Bruker spectrometer and solid-state NMR spectra (^{1}H and ^{13}C CP MAS) were acquired with a Bruker Avance 500 spectrometer.
ATR FT-IR spectra were collected in a Thermo Scientific Nicolet IS50, FTIR 6700 spectrophotometer.
Elemental Analysis Elemental analyses were performed at Mikroanalytisches Labor Pascher.
Scanning electron microscopy (SEM) was performed with a ZEISS Merlin Compact VP microscope under an accelerating voltage of 5.00 kV (Centre Technologique des Microstructures (CTμ), platform of the Claude Bernard Lyon 1 University, Villeurbanne, France).

1.3. [C_1C_4Im][Res] synthesis

To a solution of resorcinol (0.33 g, 3 mmol) in ethanol (10 mL) at room temperature, are added dropwise 1.1 g of 1-butyl-3-methylimidazolium methylcarbonate solution (37 % wt. in MeOH, 1.5 mmol). The mixture is stirred at room temperature during 24 hrs. The precipitate is washed three times with cold ethanol and dried under vacuum, yielding to 0.31 g of a white solid (82% yield).

1.4. RFs synthesis

1.4.1. RF synthesis

In absolute ethanol (64 mL)/ deionized water (160 mL) solution is dissolved resorcinol (10 mmol, 1.1g). Formaldehyde (37 % wt. in water, 40 mmol, 3 mL) is added under stirring. The mixture is heated to 100 °C during 3 days. Then the mixture is contrifugated (5000 rpm, 10 min) to recover an orange powder, that is successively washed with 3 x 20 mL of deionized water, and 3 x 20 mL of absolute ethanol. The solid is dried (P = 100 mbar, T = 70 °C, 8 hours) before characterization.

1.4.2. C_1C_4Im/RF synthesis

[C_1C_4Im][Res]:resorcinol co-crystal (0.8g) (See section 3.1) and resorcinol (0.69 g) is dissolved in absolute ethanol (40 mL)/ deionized water (100 mL) solution. Formaldehyde (30 % wt. in water, 1.1 mL) is added under stirring and then the mixture is heated to 100 °C during 8 hours. Next, the same procedure as for the RF resin was used to obtain C_1C_4Im/RF as a reddish powder.

1.5. C_1C_4Im@RF synthesis

Unfunctionalized RF (0.1 g) is suspended in 10 mL of absolute ethanol. 3 mL of 1-butyl-3-methylimidazolium methylcarbonate solution (30 % wt. in MeOH) is added and the mixture is stirred at room temperature during 4 hours. Ethanol is evaporated under reduce pressure, leading to a dark red solid, which is washed several times by ethanol until the wash solvent is no longer colored. The same procedure as for the RF resin was used to obtain C_1C_4Im@RF as a reddish powder.

1.6. Methylene blue adsorption and photodegradation

Adsorbent isotherms were done by suspension of 2 mg of resin in 15 mL of different MB solutions in dark. Concentrations of MB at equilibrium C_e were determined after 24h by measuring absorbance at 664 nm on a Perkin Elmer Lambda 35 ultraviolet/visible spectrometer. The adsorption capacity of RF resins for MB at equilibrium (q_e, mg.g^{-1}) was determined using the following equation :

$$q_e = \frac{(C_0 - C_e)V}{m_{RF}} \quad (1)$$

where V denotes the volume (L) of reaction solution and m_{RF} denotes the mass (g) of RF resin used for adsorption. Photocatalytic activities were evaluated by monitoring the degradation of MB by absorbance measurement at 664 nm along with irradiation time. 2 mg of resin are suspended in 15 ml of MB aqueous solution (5 mg.L^{-1} for RF and C_1C_4Im/RF, 30 mg.L^{-1} for C_1C_4Im@RF). The suspension is first stirred in dark for 3 h. Then the suspension is irradiated by visible light ($>$ 410 nm) (Sahi spectra Xenon light source 300 W (Max303) instrument with an ultraviolet cut-off filter). Temperature is kept at about 30°C during irradiation.

2. Results and discussion

2.1. Synthesis and characterization of [C_1C_4Im][Res]:resorcinol co-crystal

The synthesis led to the formation of a white solid, formed by the expected [C_1C_4Im][Res] co-crystallized with resorcinol, in a 1:1 stoichiometry (noted [C_1C_4Im][Res]:resorcinol) confirmed by NMR (See *Supp.Info.*), with a 82 % yield. Intriguingly, we obtained the same solid composition with other starting material ratios (using the same protocol but with [C_1C_4Im][$MeOCO_2$]:resorcinol 0.5:1 to 2:1), demonstrating a great stability of this 1:1 composition.
Single crystals obtained by crystallization through a slow evaporation of EtOH from a saturated solution in few days were analyzed by X-Ray diffraction. [26] (See Fig. 2)

The XRD structure confirms the stoichiometry: imidazolium cation and resorcinate anion aromatic rings lie in nearly parallel planes, while the resorcinol molecules lie in almost perpendicular planes (see Fig. 2). In this particular structure, one can identify three types of intermolecular bond implied in this solid formation:

- Hydrogen bonds that occur only between hydroxylate and hydroxyl groups of resorcinol and resorcinate moieties. Each O^- of resorcinate forms hydrogen bonds with three adjacent hydrogen, from both resorcinol and

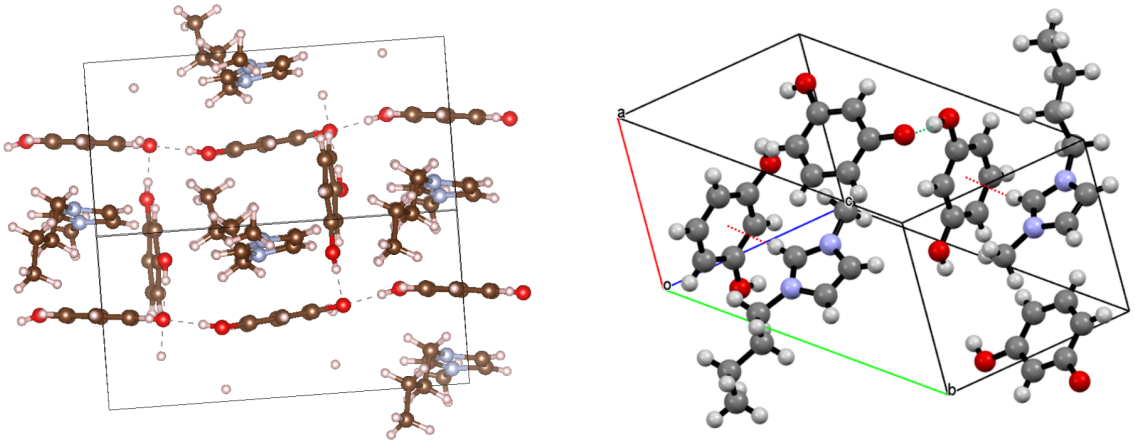

Figure 2. *Crystal structure of [C_1C_4Im][Res]:resorcinol cocrystal obtained by single crystal XRD. Left : overview of crystal structure. Right : two cells of the crystal structure: the dashed red lines represent the C-H - π interactions between imidazolium cations and resorcinol molecules*

resorcinate. No hydrogen bond is formed between imidazolium and resorcinate or resorcinol.

- Aromatic donor–acceptor interactions (π^+-π^- interactions)[27] between imidazolium cations and resorcinate anions (interplanar distance = 3.87 Å). π^+-π^+ interactions, between imidazolium cations, are common in imidazolium-based ionic liquids.[28,29] By contrast, π^+-π^- interactions in imidazolium ionic compounds have not been described so far to our knowledge. Actually, very few imidazolium-based compounds with an aromatic anions has been extensively described. Nethertheless, in case of phenolate imidazoliums,[30] or tetraphenylborate butyl methylimidazolium ionic pairs,[31] no π^+-π^- interactions were observed in XRD structures, where hydrogen bond or C-H - π interactions predominate. It should be noted that only resorcinol anions, and no resorcinol molecules, participate in these interactions.
- C-H - π interactions between the N-CH-N proton (C2) of the imidazolium cation and the resorcinol ring. C-H - π interactions can be very weak in case of non polarized C-H bonds, or similar to classical hydrogen bonds in case of strongly polarized C-H bonds, as in $CHCl_3$.[32] They are frequently described in supramolecular complexes[33,34] and in molecular recognition.[35–37] As butyl-methylimidazolium cation is very frequently used in ionic liquids,[38] the study of interactions between this ion and the other compounds is particularly important for understanding the physico-chemical properties of ionic liquids, and the imidazolium N-CH-N hydrogen is often involved in hydrogen bond with the anion[28,29,39–43]. Surprisingly, in the case of the cocrystal [C_1C_4Im][Res]:resorcinol, the proton of C2 of the imidazolium cation is not involved in any hydrogen bond, but only in a C-H - π interaction with the resorcinol (and not the resorcinate). Indeed, the distance between C2 proton and the centroid of the resorcinol ring is as short as of 2.36 Å . The angle between the imidazolium plane and the resorcinol plane is 99.5 degrees, in a typical "T-shape" geometry (see Fig. 2). To our knowledge, C-H - π interactions involving butyl-methylimidazolium cation were previously described only by Dupont *et al.* between butyl methylimidazolium and tetraphenylborate anion.[31]

2.2. Synthesis of resorcinol-formaldehyde resins

2.2.1. Catalyst-free synthesis and characterization of RFs

We perform the synthesis of RF particles with a well known methodology in ethanol:water mixture,[44] but without using any catalyst, in order not to alter the composition of the resin, and notably to avoid the presence of residual metals (Na, K), carbonate, or ammonia from the classically used catalysts.[45] Consequently, time reactions are longer (3 days), and the dispersity of the RFs particles is higher than the previously reported preparation. However, we believe that the absence of residual traces of these catalysts will be necessary for an accurate assessment of the photocatalytic properties of RFs. Despite the absence of any catalyst nor tailoring agents, SEM images of RFs show spherical particles with diameters mainly from 300 to 800 nanometers (mean diameter = 550 nm. Fig. 3 a.), with few bigger particles ($\approx 1\ \mu$m) similar in shape with semiconductive RF particles discribed by Shirashi *et al.*[12] ^{13}C CP/MAS NMR, IR and UV-Visible spectra are also similar, as well as the energy gap Eg (Eg = 2.04 eV, calculated using the Tauc Method (see Fig. 4 and *Supp. Info.*). Elemental analysis confirms the absence of nitrogen (see Table 1). To assess the dispersity of the sample, we determine the polydispersity index (PDI) by the formula :

$$PDI = \frac{\sigma^2}{Z^2} \tag{2}$$

where σ is the standard deviation of particles diameters, and Z the mean diameter (determined by direct measurement of 200 particles diamters on SEM pictures). We find PDI=0.02 without taking into account of the few bigger particles, showing a relatively monodisperse distribution.

2.2.2. Synthesis and characterization of C_1C_4Im/RF

When [C_1C_4Im][Res]:resorcinol solid is used as co-precursor together with resorcinol and formaldehyde, the time reaction is considerably shorter (few hours), showing that [C_1C_4Im][Res]:resorcinol acted as well as a reactant and a basic catalyst. The resulting solid is a reddish powder.

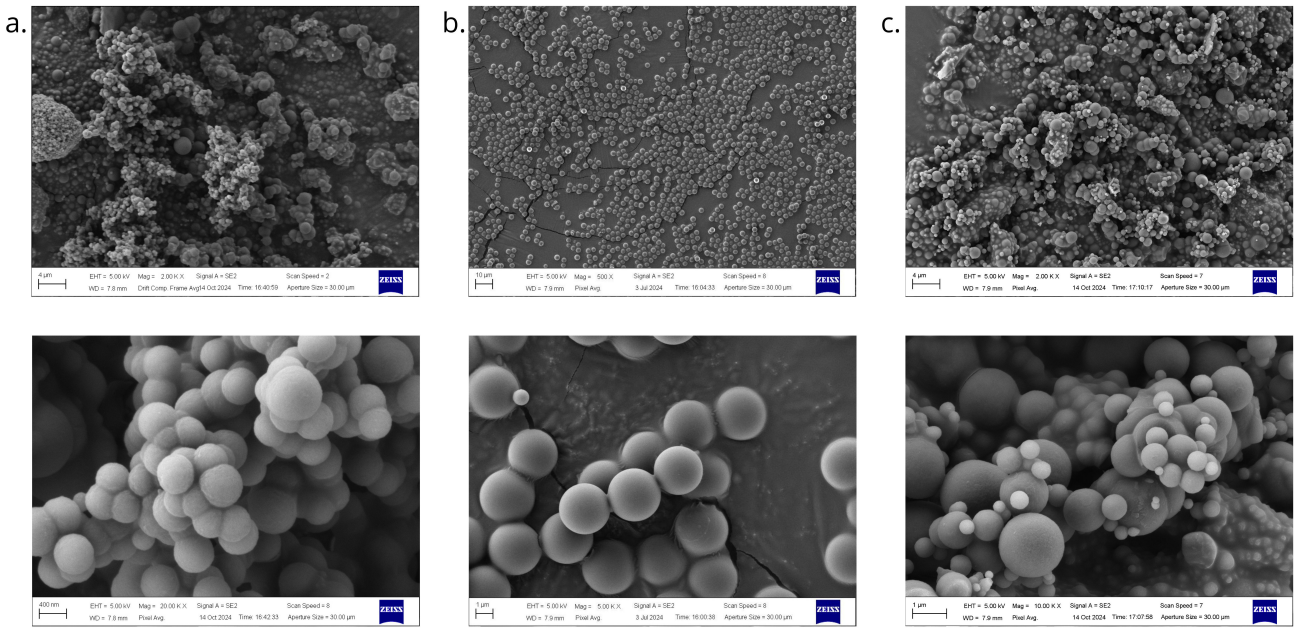

Figure 3. SEM images of the synthesized RF (top images : overview, bottom images : details). a: unsubstituted RF. b: pre-functionalized C_1C_4Im/RF. c: post-functionalized C_1C_4Im@RF

When compared to the ATR-FTIR spectrum of unsubstituted RF, the one from C_1C_4Im/RF exhibits new absorption bands in 700-900 cm^{-1} and 2900-3200 cm^{-1} regions that are characteristics of C-H vibrating and stretching of $[C_1C_4Im]$ cation (Fig. 4b.). ^{13}C CP/MAS NMR spectrum confirms the presence of $[C_1C_4Im]$, as the new bands correspond to aliphatic carbon of the methyl and butyl chain of the cation (Fig. 4a.). Elemental analysis also confirms the substantial presence of $[C_1C_4Im]$ cation in C_1C_4Im/RF, as the N:C ratio is 5.3 % and nitrogen element only comes from imidazolium ring (Table 1. The energy gap of C_1C_4Im/RF, calculated with the Tauc method, is significantly lower than the unfunctionalized RF one, at 1.78 eV (Fig. 4c., Table 1). SEM pictures of C_1C_4Im/RF show spheric particles, with a mean diameter of 3.1 µm, near from 10 times bigger than non-functionalized RF. Remarkably, the size distribution of these particles is considerably more uniform (PDI= 0.003 calculated from the direct measurement of 200 particle diameters on SEM pictures) Fig. 3 c.)), which indicates a great monodispersity of the sample, confirming the tayloring role of $[C_1C_4Im][Res]$ during the synthesis.

2.2.3. Synthesis and characterization of C_1C_4Im@RF

The treatment of RF with $[C_1C_4Im][MeOCO_2]$ leads to a dark red powder. Elemental analysis shows that the amount of incorporated $[C_1C_4Im]$ in the new material is almost doubled compared to C_1C_4Im/RF (Table 1). ATR-FTIR spectrum shows, as in C_1C_4Im/RF spectrum, the same bands that can be attributed to $[C_1C_4Im]$ cation with expected enhanced intensities. In ^{13}C CP/MAS NMR, bands that correspond to the alkyl chains of $[C_1C_4Im]$ are not only more intense, but also particularly sharper, due to an averaging of dipolar couplings (Fig. 4a.). It indicates an increase of the mobility of these alkyl chains in C_1C_4Im@RF compared to C_1C_4Im/RF, which is expected given the post-functionalization strategy, where functionalized sites are probably mainly located on the surface of the particles. The calculated energy gap is slightly lower than the Eg value for C_1C_4Im/RF (1.72 eV) (Fig. 4 c.). SEM pictures show that the post-treatment of RF changes the size distribution of the particles : one can see more particles with a diameter larger than 1 μm, and a part of the smaller ones are fused. That can be explained by the basic properties of $[C_1C_4Im][MeOCO_2]$ that can degrade RF structure, as it has already been studied for alkaline solutions exposition of resorcinol-formaldehyde resins (Fig. 3 c.).[46]. To verify this hypothesis, we synthesized again C_1C_4Im@RF, waiting 3 days before washing the red solid obtained by evaporation of solvents after treatment by $[C_1C_4Im][MeOCO_2]$. The SEM pictures (see *Supp. Info.*, Fig. S6) clearly show a high degree of degradation, with no more spherical particles.

Table 1. Properties of synthesized RF

Resins	RF	C_1C_4Im/RF	C_1C_4Im@RF
N:C ratios[a]	0 %	5.3 %	8.5 %
Eg (eV)[b]	2.05	1.78	1.72
PDI	0.02	0.003	n.d.[c]
BET area ($m^2.g^{-1}$)	5.4	1.5	4.9

[a]Determined by elemental analysis. [b]Determined by Tauc method. [c]Not determined : particles are partially degraded.

2.3. Properties of C_1C_4Im/RF and C_1C_4Im@RF

As example of photocatalysis, we study the methylene blue photodegradation catalyzed by our three new resorcinol-formaldehyde resins: because of its widespread industrial use, and its potential harmfulness to human health and the environment, the cationic dye methylene blue (MB) has been frequently used as a model to evaluate the photocatalytic and adsorbent properties of new materials.[47–49]

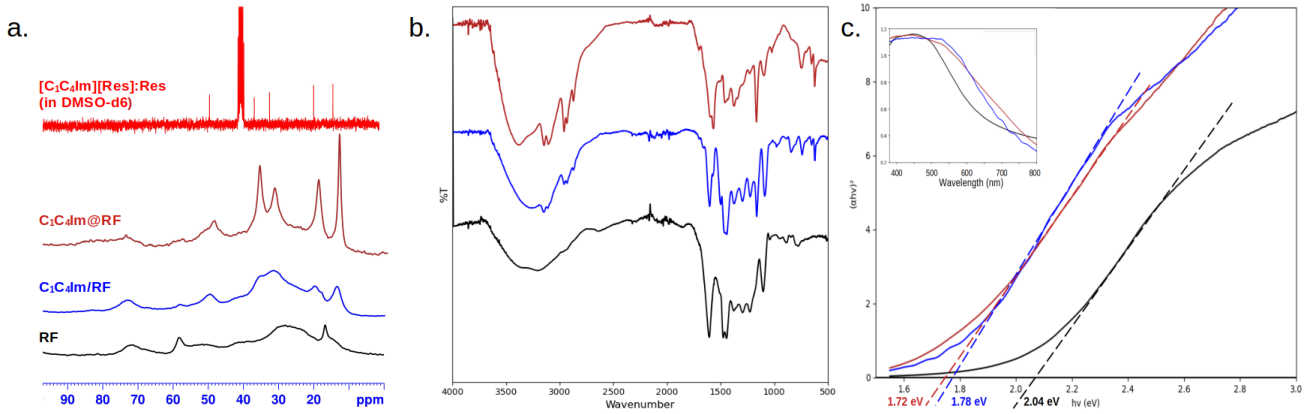

Figure 4. a. ^{13}C CP MAS NMR spectra (0 - 100 ppm) of synthesized RFs compared to ^{13}C NMR spectrum of $[C_1C_4Im][Res]$:resorcinol. b. FTIR spectra of synthesized RFs. c. Tauc plot for synthesized RFs. In black: unsubstitued RF, blue: C_1C_4Im/RF, dark red: $C_1C_4Im@RF$.

2.3.1. Adsorbent properties

During these experiments, we first found that the adsorbent properties in the dark of RF and C_1C_4Im/RF in one hand, and of $C_1C_4Im@RF$ in the other, differ significantly. Adsorption isotherms at 20°C of MB on RF and C_1C_4Im/RF followed the Langmuir model ($R^2 > 0{,}99$), indicating that the surface of these two types of particles are homogeneous and a monolayer adsorption of MB. They present a maximum adsorption capacity q_{max} of the same order of magnitude (respectively, 43 $mg.g^{-1}$ and 45 $mg.g^{-1}$). In contrast, $C_1C_4Im@RF$ presents excellent adsorption of MB and adsorption isotherm is in excellent agreement with the Freundlich model ($R^2 > 0{,}99$), indicating multi-layer adsorption and/or heterogeneous surface. q_{max} (calculated from Langmuir equation) is 20 times higher (863 $mg.g^{-1}$). This result is unexpected, considering that $C_1C_4Im@RF$ is not micro- or mesoporous nor has a large surface area : for comparison, q_{max} is of the same order of magnitude as activated carbon which has a BET surface area more than 100 times higher.[48] The agreement with Freundlich model instead of Langmuir model demonstrates that the mechanism of adsorption of MB on $C_1C_4Im@RF$ surface is not the same as on RF or C_1C_4Im/RF. RF post-modification by $[C_1C_4Im][MeOCO_2]$ creates ionic bonds between hydroxylate groups on the resin surface and imidazolium cations. It can be assumed that these exchange readily with the MB cations, and anionic sites provide a favorable electrostatic environment for multilayer MB absorption.[50]

Kinetic experiments showed efficient catalysis of MB photodegradation by RF, C_1C_4Im/RF and $C_1C_4Im@RF$. For RF, we observe a higher initial rate ($C_0 = 5$ $mg.L^{-1}$, v_0=1 $mg.L^{-1}.min^{-1}$), followed by a pseudo-second order kinetic. For the two imidazolium-modified RFs, MB degradation occurs directly with pseudo-second order kinetic. Rate constant is increase by a factor of 2.1 for C_1C_4Im/RF (resp. 1.5 for $C_1C_4Im@RF$) showing a direct effect of the $[C_1C_4Im]$ cations. However we suppose that photocatalytic rates is limited by the small surface area of RF particles, and more studies are needed to elucidate the photocatalysis mechanism, and the behavior difference modified and unmodified RF resins.

Conclusion

We have synthesized new resorcinol-formaldehyde spheric particles, without catalyst, via pre- and post-functionalisation strategies, using the commercial reagent butyl methylimidazolium methylcarbonate, demonstrating the effectiveness of the use of methylcarbonate ionic liquids as precursor for new functionalized materials. The pre-functionalisation strategy led to monodisperse RF particles, which could be notably used for the production of new size-controlled carbon microparticle materials. In addition, single crystal XRD structure of the new ionic compounds $[C_1C_4Im][Res]$ which co-crystallize with resorcinol opens the way to a better understanding of intermolecular interactions in ionic compounds, including π^+-π^- and C-H-π interactions, which could exist in certain ionic liquid medium. Post-functionalization enables imidazolium cations to be grafted onto the particle surface in larger quantities and with greater mobility, although the structure of RF particles is partially degraded. These two synthetic strategies led to lower band gaps of these new resins compared to the classical RF, that makes them attractive for photocatalysis applications. To illustrate it, we used RF and $[C_1C_4Im]$-modified RFs to photocatalyze methylene blue degradation. $C_1C_4Im@RF$ and C_1C_4Im/RF showed improved catalytic properties compared to RF particles cataysis. Moreover, $C_1C_4Im@RF$ showed impressive MB adsorbent performance. This first set of experiments shows that imidazolium modified RFs have great potential for pollution control, thanks to their dual capacity for adsorbing organic cations and for their photodegradation. Further work will give us a better understanding of the mechanisms involved in these two phenomena, in the aim of improving their performances and exploring the possibility of a synergy between the adsorbent and photocatalytic properties.

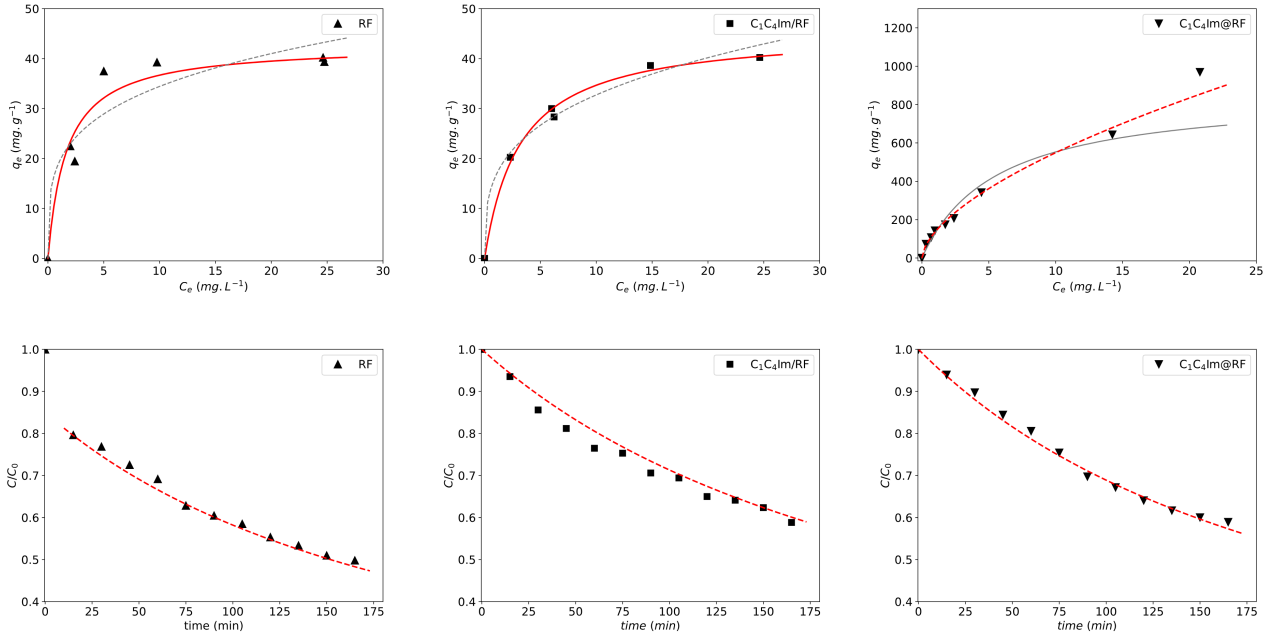

Figure 5. Top : methylene blue absorption capacity (q_e) *vs.*Ce at 20°C for RF, C_1C_4Im/RF and C_1C_4Im@RF. Solid line : Langmuir model, dashed line : Freundlich Model. Bottom : photodegradation kinetics at 30°C : C/C_0 *vs.* time (min). Dashed line : pseudo-second order kinetic. For all graphs : best model is plotted in red.

Table 2. adsorbent and photocatalytic properties

		RF	C_1C_4Im/RF	C_1C_4Im@RF
Adsorption Isotherm	*Langmuir model*			
	R^2	*0.994*	*0.998*	*0.92*
	q_{max} $(mg.g^{-1})$	43	45	863
	K_L	0.604	0.315	0.179
	Freundlich model			
	R^2	*0.96*	*0.73*	*0.99*
	n	3.97	3.38	1.66
	K_F	19.3	16.6	8.5
Adsorption kinetic *Pseudo 2d order*	R^2	*0.97*[a]	*0.98*	*0.99*
	k $(L.mg^{-1}.min^{-1})$	0.00064	0.0031	0.0024
Photodegradation kinetic *Pseudo 2d order*	R^2	*0.98*	*0.99*	*0.99*
	k $(L.mg^{-1}.min^{-1})$	0.0011	0.00237	0.0017

[a] Without initial rate between t = 0 and 15 min.

Acknowledgements

The authors are grateful for the financial support of CSC (Chinese scientific Council) and from Ambassade de France à Jerusalem. They thank Pierre-Yves Dugas for SEM, Kai C. Szeto for elemental analysis measurement.

Conflict of Interest

There are no conflicts to declare.

Keywords: Resorcinol-Formaldehyde Resin • Butylmethylimidazolium-modified materials • Photocatalysis • Absorbent materials •Methylene Blue Removal

References

[1] R. B. Durairaj, Resorcinol Based Resins and Applications, in *Resorcinol: Chemistry, Technology and Applications*, pages 179–261, Springer, Berlin, Heidelberg **2005**.
[2] Q. Ren, R. Sun, D. Feng, H. Ru, W. Wang, C. Zhang, *Colloids and Surfaces A: Physicochemical and Engineering Aspects* **2022**, *647*, 129192.
[3] F. Li, L. Xie, G. Sun, Q. Kong, F. Su, Y. Cao, J. Wei, A. Ahmad, X. Guo, C.-M. Chen, *Microporous and Mesoporous Materials* **2019**, *279*, 293.
[4] G. Zhang, C. Ni, L. Liu, G. Zhao, F. Fina, J. T. S. Irvine, *Journal of Materials Chemistry A* **2015**, *3*, 15413.
[5] Y. Zan, M. Zhai, Y. Ni, *Journal of Materials Science: Materials in Electronics* **2018**, *29*, 10061.
[6] X. Li, J. He, J. Lu, Y. Zhou, Y. Zhou, *Journal of Hazardous Materials* **2022**, *424*, 127650.
[7] C. Zhao, X. Wang, S. Ye, J. Liu, *Solar RRL* **2022**, *6*, 2200427.
[8] X. Lv, H. Yuan, K. Sun, W. Shi, C. Li, F. Guo, *Molecules* **2024**, *29*, 1514.
[9] L. Zhang, P. Su, Y. Wang, R. Djellabi, J. Zhao, *Chemosphere* **2024**, *347*, 140620.
[10] B. Liu, L. Yan, J. Wen, X. Liu, F. Duan, B. Jia, X. Liu, G. Ke, H. He, Y. Zhou, *New Journal of Chemistry* **2022**, *46*, 17809.
[11] S. Zhou, Y. Cai, J. Zhang, Y. Liu, L. Zhou, J. Lei, *ACS Sustainable Chemistry & Engineering* **2022**, *10*, 14464.
[12] Y. Shiraishi, T. Takii, T. Hagi, S. Mori, Y. Kofuji, Y. Kitagawa, S. Tanaka, S. Ichikawa, T. Hirai, *Nature Materials* **2019**, *18*, 985.
[13] Y. Shiraishi, T. Takii, T. Hagi, S. Mori, Y. Kofuji, Y. Kitagawa, S. Tanaka, S. Ichikawa, T. Hirai, *Nature Materials* **2019**, *18*, 985.
[14] Y. Shiraishi, T. Hagi, M. Matsumoto, S. Tanaka, S. Ichikawa, T. Hirai, *Communications Chemistry* **2020**, *3*, 1.
[15] Y. Shiraishi, M. Matsumoto, S. Ichikawa, S. Tanaka, T. Hirai, *Journal of the American Chemical Society* **2021**, *143*, 12590.
[16] Y. Shiraishi, K. Miura, M. Jio, S. Tanaka, S. Ichikawa, T. Hirai, *ACS Materials Au* **2022**, *2*, 709.
[17] X. Li, Q. Zheng, X. Wang, Q. Zheng, Y. Zhang, Y. Cong, S.-W. Lv, *Journal of Materials Chemistry A* **2024**, *12*, 8420.
[18] C. Shi, C. Lin, X. Huang, Q. Wu, H. Ge, Y. Yang, *Journal of Materials Science: Materials in Electronics* **2024**, *35*, 1070.
[19] O. Czakkel, E. Geissler, I. M. Szilágyi, K. László, *Nanomaterials and the environment* **2013**, *1*, 23.
[20] C. Huang, W. Dai, S. Deng, Y. Tian, X. Liu, J. Lin, H. Chen, *Chinese Chemical Letters* **2024**, *35*, 109429.
[21] X. Liang, *Kinetics and Catalysis* **2013**, *54*, 724.
[22] M. Tiano, R. Clark, L. Bourgeois, M. C. Gomes, *Green Chemistry* **2023**, *25*, 2541.
[23] R. Matsuno, Y. Kokubo, S. Kumagai, S. Takamatsu, K. Hashimoto, A. Takahara, *Macromolecules* **2020**, *53*, 1629.
[24] S. A. M. Noor, J. Sun, D. R. Macfarlane, M. Armand, D. Gunzelmann, M. Forsyth, *Journal of Materials Chemistry A* **2014**, *2*, 17934.
[25] A. R. Zanatta, *Scientific Reports* **2019**, *9*, 11225.
[26] Deposition Number 2384665 (for $[C_1C_4Im][Res]$) contains the supplementary crystallographic data for this paper. These data are provided free of charge by the joint Cambridge Crystallographic Data Centre and Fachinformationszentrum Karlsruhe Access Structures service www.ccdc.cam.ac.uk/structures.
[27] C. R. Martinez, B. L. Iverson, *Chemical Science* **2012**, *3*, 2191.
[28] R. P. Matthews, T. Welton, P. A. Hunt, *Physical Chemistry Chemical Physics* **2014**, *16*, 3238.
[29] R. P. Matthews, T. Welton, P. A. Hunt, *Physical Chemistry Chemical Physics* **2015**, *17*, 14437.
[30] N. Kuhn, C. Maichle-Mößmer, M. Steimann, *Zeitschrift für Naturforschung B* **2009**, *64*, 835.
[31] J. Dupont, P. A. Z. Suarez, R. F. De Souza, R. A. Burrow, J.-P. Kintzinger, *Chemistry – A European Journal* **2000**, *6*, 2377.
[32] S. Tsuzuki, K. Honda, T. Uchimaru, M. Mikami, K. Tanabe, *The Journal of Physical Chemistry A* **2002**, *106*, 4423.
[33] K. Kobayashi, Y. Asakawa, Y. Kikuchi, H. Toi, Y. Aoyama, *Journal of the American Chemical Society* **1993**, *115*, 2648.
[34] F. Biedermann, H.-J. Schneider, *Chemical Reviews* **2016**, *116*, 5216.
[35] P. V. Balaji, *Mini-Reviews in Organic Chemistry* **2011**, *8*, 222.
[36] V. Spiwok, *Molecules* **2017**, *22*, 1038.
[37] L. L. Kiessling, R. C. Diehl, *ACS Chemical Biology* **2021**, *16*, 1884.
[38] D. Zheng, L. Dong, W. Huang, X. Wu, N. Nie, *Renewable and Sustainable Energy Reviews* **2014**, *37*, 47.
[39] K. Dong, S. Zhang, D. Wang, X. Yao, *The Journal of Physical Chemistry A* **2006**, *110*, 9775.
[40] T. Takamuku, T. Tokuda, T. Uchida, K. Sonoda, B. A. Marekha, A. Idrissi, O. Takahashi, Y. Horikawa, J. Matsumura, T. Tokushima, H. Sakurai, M. Kawano, K. Sadakane, H. Iwase, *Phys. Chem. Chem. Phys.* **2018**, *20*, 12858.
[41] A. A. Rodríguez-Sanz, E. M. Cabaleiro-Lago, J. Rodríguez-Otero, *Organic & Biomolecular Chemistry* **2015**, *13*, 7961.
[42] Y.-L. Wang, A. Laaksonen, M. D. Fayer, *The Journal of Physical Chemistry B* **2017**, *121*, 7173.
[43] L. Zhang, L. Wei, S. Zhai, D. Zhao, J. Sun, Q. An, *Chinese Journal of Chemical Engineering* **2020**, *28*, 1293.

[44] J. Liu, S. Z. Qiao, H. Liu, J. Chen, A. Orpe, D. Zhao, G. Q. M. Lu, *Angewandte Chemie International Edition* **2011**, *50*, 5947.
[45] E. Martin, M. Prostredny, A. Fletcher, *Gels* **2021**, *7*, 142.
[46] I. M. K. Lawrence M. Pratt, Rosmarie Szostak, J. Bibler, *Journal of Macromolecular Science, Part A* **1997**, *34*, 281.
[47] E. Santoso, R. Ediati, Y. Kusumawati, H. Bahruji, D. O. Sulistiono, D. Prasetyoko, *Materials Today Chemistry* **2020**, *16*, 100233.
[48] M. Rafatullah, O. Sulaiman, R. Hashim, A. Ahmad, *Journal of Hazardous Materials* **2010**, *177*, 70.
[49] I. Khan, K. Saeed, I. Zekker, B. Zhang, A. H. Hendi, A. Ahmad, S. Ahmad, N. Zada, H. Ahmad, L. A. Shah, T. Shah, I. Khan, *Water* **2022**, *14*, 242.
[50] L.-L. Zhang, A. Zaoui, W. Sekkal, *Journal of Water Process Engineering* **2024**, *57*, 104651.

Entry for the Table of Contents

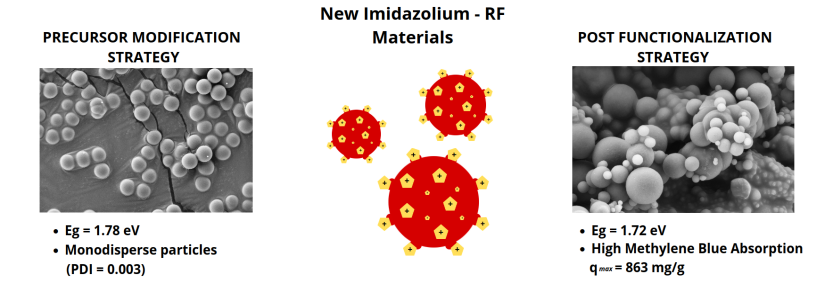

The order in the recipe matters ! New semiconductive resorcinol-formaldehyde resins (RFs) have been synthesized using butyl-methylimidazolium methylcarbonate ionic liquid. Depending on the pre- or postfunctionalization strategies, new materials present different benefits: dispersity control, variation of the band gap and significant improvement the absorption properties toward methylene blue.